The effect of the drying temperature on water porosity and gas permeability of recycled sand mortar

Aiman Yacoub, Assia Djerbi Tegguer, Teddy Fen Chong

The effect of the drying temperature on water porosity and gas permeability of recycled sand mortar

Aiman Yacoub, Assia Djerbi Tegguer, Teddy Fen Chong

Version of Record: https://www.sciencedirect.com/science/article/pii/S0950061819310165
Manuscript_1c9ea22f5f60b5b356fc6f667fd8a491

The effect of the drying temperature on water porosity and gas permeability of recycled sand mortar

Aiman YACOUB, Assia DJERBI, Teddy FEN-CHONG

Université Paris-Est, MAST, FM2D, IFSTTAR, 14-20 Boulevard Newton, Cité Descartes, Champs sur Marne, F-77447 Marne la Vallée Cedex 2, France

assia.djerbi@ifsttar.fr

ABSTRACT

The main purpose of this study is to determine the effect of the drying temperature on the durability indicators such as water porosity and gas permeability of mortar made of recycled sand. A relationship between experimental parameters such as mass loss and water absorption and durability indicators has been established. Mortars made of recycled sand (M-RS) and natural sand (M-NS) were fabricated and then tested after a pre-treatment at different temperatures (60°C, 80°C and 105°C). Water porosity and gas permeability were determined then at each temperature range (60°C, 80°C and 105°C) using the same specimen. Results show that the increase in the drying temperature from 60°C to 105°C does not influence the water porosity of M-RS as much as the gas permeability. Second, the increase in the gas permeability with the drying temperature is not only due to the water evaporation but also to the micro-cracks created during the drying process. Finally, pre-treating samples at 105°C as suggested by the standard methods affects the microstructure of M-RS and leads to false results; a pre-treatment temperature of 60°C is more appropriate in the case of mortars made of RS.

Key words: recycled sand, water porosity, gas permeability, drying temperature, durability properties

1. Introduction

Construction and demolition waste are widely used nowadays in the construction and civil engineering fields, as road construction and maintenance and as recycled concrete aggregates

(RCA) to replace the natural aggregates (NA) in fabricating new concrete. Unfortunately, a total substitution of the NA by the RCA is not yet possible due to the properties of the RCA (high porosity, high water absorption coefficient, etc.) [1–3]. According to Xiao et al [4], only a 30% replacement of the NA by the RCA is achievable, whereas the European standards NF EN 206+A1 [5], state that the replacement ratio of coarse RCA (characterized according to EN 12620) can reach up to 50% in some cases.

RCA contains about 20-25% in mass of adherent cement paste [6–9] which affects the microstructure of the RCA compared to the NA. Replacing NA by RCA in fabricating new concrete negatively affects the performance and the pore structure of the recycled aggregate concrete (RAC). High temperature enhances the problem facing the replacement of NA by RCA. While heating NA to 110°C for drying purposes is very common, the microstructure of the RCA is affected at this temperature due to the adherent cement paste [10]. For a temperature range between 80°C and 105°C, a part of the bound water next to the evaporable water escapes [11,12]. The dehydration of the C-S-H starts off within this range of temperature [13] along with the dehydration of ettringite that triggers for a temperature above 75°C [14].

Despite the difference in properties between RCA and NA, standard methods designed for normal concrete and mortars are still used to evaluate the durability indicators of RAC. Within this context, most of the experiments developed to investigate the durability properties of concrete, such as water porosity and gas permeability, require a pre-treatment of the specimen at 105°C. Durability indicators are very important as they indicate the ability of the concrete to withstand the effects of time and external environment. Hence heating RAC at 105°C before any durability test may lead to false results.

In this paper, water porosity and gas permeability of M-RS (fraction 1-4 mm) are determined under different drying temperatures (60°C, 80°C and 105°C) in order to investigate the temperature effect on the results obtained. Both indicators are compared to the ones of M-NS.

In this way, an improved choice of the temperature for evaluating the durability properties of M-RS can be made.

2. Materials

CEM I 52.5 N CE CP2 NF is the type of cement used in this study; its chemical composition is given in Table 1. The recycled sand used in this study was provided by the French national project Recybeton as a fraction of 0-4 mm. The sand received (natural and recycled) is sieved between 1 and 4 mm before any use. Fig. 1 shows that the particle size distributions of both sands are similar. Knowing that RS has a heterogeneous microstructure and its properties depend on the source of supply, it is important to determine its characteristics prior to any use. Physical properties of the RS and the NS such as compactness, the water absorption coefficient (WAC) and density are determined. The method used to determine the WAC and the density of the sand is the one developed by Yacoub et al [15] since the standard method EN 1097-6 underestimates these values [16]. The results are shown in Table 2; the WAC of the RS is much higher than the NS, while the density and compactness of the RS are lower than the NS. This is expected since the RS is more porous than the NS. The attached mortar content is evaluated using a chemical treatment based on salicylic acid [17].

A total volume substitution of the NS by RS is carried out in this study.

SiO_2	Al_2O_3	Fe_2O_3	CaO	MgO	SO_3	K_2O	Na_2O	S^-	Cl^-	CO_2	Free CaO	Ignition loss
20.2%	5.1%	3%	64%	1%	3.1%	0.75%	0.21%	0%	0.03%	0.4%	1.6%	0.7%

Table 1 : The chemical composition of the cement

	WAC (%)	Density (kg/m^3)	Compactness	Porosity (%)	Attached mortar content (%)
Recycled Sand	10.91	2440	0.56	20.85	25,8
Natural Sand	2.3	2530	0.63	7	-

Table 2: Physical properties of the RS and NS measured following the developed method in [15]

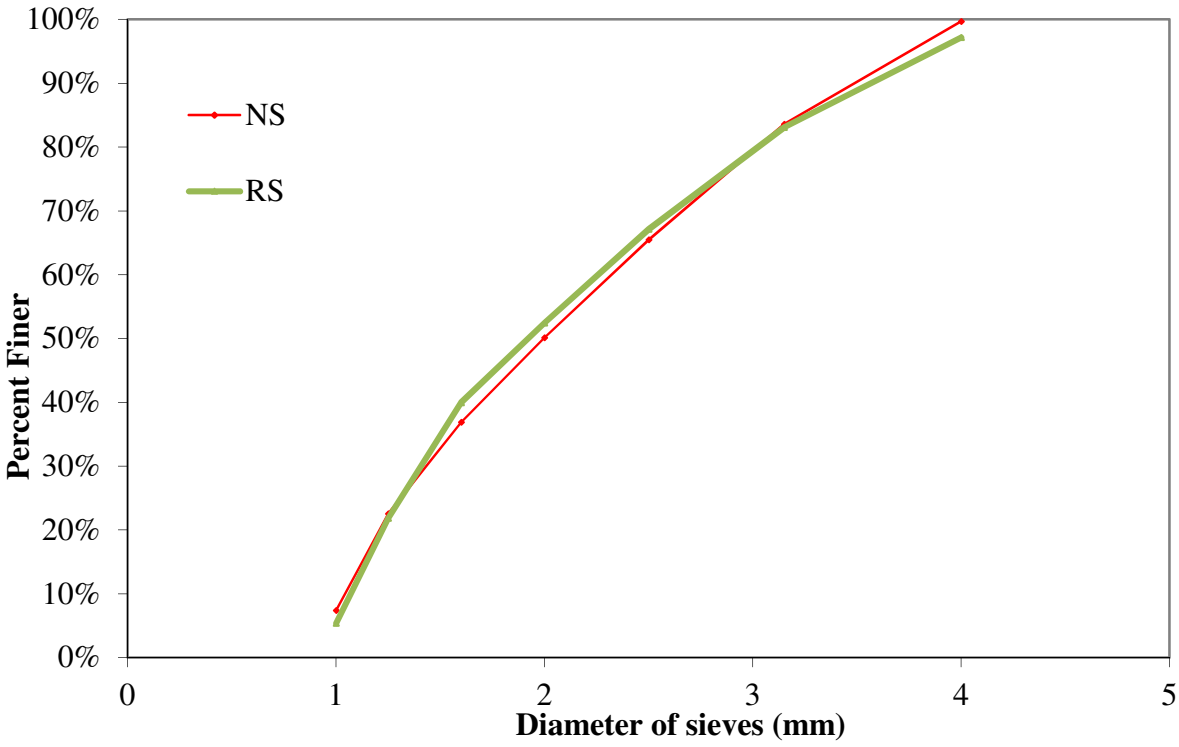

Fig. 1: The particle size distribution of the RS and NS

3. Experimental program

3.1 Mixing procedure of mortar

The mixing procedure is done according to the standard NF EN 196-1 [18]. For all mixes, the W/C ratio used is 0.5 and the S/C ratio is 3. Two types of mortars are fabricated for this study: the reference mortar made of natural sand and mortar with 100% replacement of natural sand by recycled sand. Both sands are used in the dry state. Table 3 presents the composition of the mortars. Cylindrical specimens with a diameter of 5 cm and 20 cm height were cast and subjected to a water immersion curing for 90 days. After the curing period, specimens with a diameter of 5 cm and 5 cm thickness were extracted from the center of the cylinder using a disc saw. The same specimens undergo both tests: water porosity and gas permeability. The results presented are the average of three specimens tested.

	Cement (g)	Recycled Sand (g)	Natural Sand (g)	W (g)	Water for absorption added into the mix (g)
M-RS	1,400	4,051	-	700	442
M-NS	1,400	-	4,200	700	97

Table 3: The compositions of mortars fabricated

3.2 Water porosity

The water porosity test was carried out according to the standard method [19] with some modifications in order to study the effect of the drying temperature on mortar made of recycled sand. The specimen is dried at 105°C at the end of the test and not at first as recommended in the standard method in order to start with lowest temperature without damaging the microstructure. In addition to the water porosity value obtained at 105°C, we calculated the water porosity of the specimen at the temperature of 60°C and 80°C. The water porosity is calculated as follows:

$$P = \frac{M_{sat} - M_{dry\ at\ T}}{M_{sat} - M_{water}} \times 100 \quad (1)$$

M_{sat}: the mass (g) of the saturated specimen in the air,

$M_{dry\ at\ T}$: the mass (g) of the dried specimen at the desired temperature,

M_{water}: the mass (g) of the saturated specimen under water.

3.3 Gas permeability

In this article, permeability of mortar to nitrogen was determined using the CEMBUREAU method [20]. The temperatures recommended to dry the specimen before carrying out the test were modified in this research. The gas permeability test was done for three different drying temperatures: 60°C, 80°C and 105°C. The underlying principle used for this test is the Hagen-Poiseuille relation for laminar flow of a compressible fluid through a porous body under steady-state condition. Hagen-Poiseuille equation below allows determining the specific permeability coefficient:

$$K_a = \frac{2.Q.P_{atm}.L.\mu}{A.(P^2 - P_{atm}^2)} \quad (2)$$

Where *Q:* volume flow rate of the fluid (m^3/s), L*:* thickness of the specimen (m) = 0.051m, *A:* cross-sectional area of the specimen (m^2) = 7.854×10^{-3} m^3, μ*:* dynamic viscosity of the fluid (Nitrogen) at 20°C (Pa.s) = 1.76×10^{-5} Pa.s, P_{atm}*:* atmospheric pressure (Pa) = 101 325 Pa, *P:* inlet pressure (Pa).

Having *Ka* for different inlet pressures, the intrinsic permeability of the mortar can be calculated using the method of Klinkenberg [21]:

$$K = K_{int}\,(1 + \frac{\beta}{P_m}) \quad (3) \qquad P_m = \frac{P_0 + P_{atm}}{2} \quad (4)$$

Where $P_{0:}$ atmospheric pressure (Pa), β: Klinkenberg constant and $\beta.K_{int}$: the slope of the line of Klinkenberg.

The experimental program carried out in this study is explained in Fig. 2

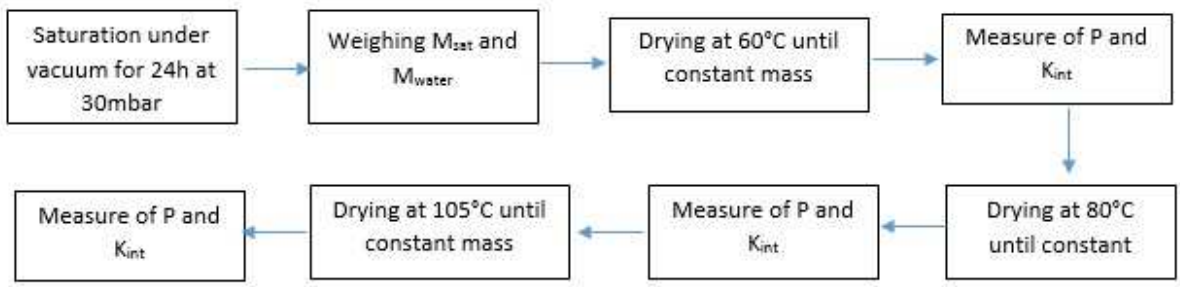

Fig. 2: Experimental process

3.4 Mass loss

The mass loss of mortars at different temperature ranges is measured. The percentage of mass loss between two ranges of temperatures ($M_{Tinitital}$ and M_{Tfinal})is calculated after the stabilization of the mass at the desired temperature using the following equation:

$$\text{Mass loss } (\%) = \frac{M_{Tfinal}}{M_{Tinitial}} \times 100 \quad (5)$$

Where : M_{Tfinal} = The higher temperature and $M_{Tinitial}$ = the lower temperature

3.5 The dynamic modulus of elasticity (E)

The dynamic modulus of elasticity is determined nondestructively on 4×4×16 cm^3 mortar specimens. The longitudinal frequency is measured using the resonance test based. E is then calculated using the following equation:

$$E = 4.\rho.L^2.F_l^2 \quad (6)$$

Where: E = the dynamic modulus of elasticity (MPa), ρ = Density (kg/m^3), L = the length of the specimen (m), F_l = Longitudinal frequency (Hz).

The dynamic modulus of elasticity is measured after drying the specimens at the following temperatures: 20°C, 60°C, 80°C and 105°C. The damage coefficient (D) which is a measure of the stiffness degradation of the specimen is calculated using the following equation:

$$D = \frac{E_{20°C} - E_T}{E_{20°C}} \quad (7)$$

$E_{20°C}$ is the dynamic modulus of elasticity of the mortar at 20°C and E_T is the dynamic modulus of elasticity after heating at temperature T (80°C and 105°C). The damage coefficient D represents the degree of micro-cracking of the specimen [22].

4. Results and discussion

4.1 Mass loss

Fig. 3 presents the mass loss of M-NS and M-RS with respect to time at different drying temperatures. The results of the percentage of mass loss are presented in 4. The major mass loss happens between 20°C and 60°C; this is due to the evaporation of the free porous water without any effect on the adsorbed water or on the microstructure of the mortar. Adsorbed water remains stable for a temperature range 65°C-80°C [13,23]. A small decrease in mass in noticed for the temperatures range 60°C-80°C and 80°C-105°C. For these ranges of temperature, mass loss is

the result from the evaporation of interlayer water from C-S-H gel [23] or loss of the bound water [24]. The escape of this water causes damages to the microstructure of the mortar. Authors in [24] found that major changes in microstructure of cement paste starts to happen at temperatures ranged between 80-105°C and the cause of these changes is the departure of the interlayer water from the C-S-H gel. In order to determine the contribution of the sand in the mass loss of the mortar, NS and RS used to fabricate mortars are dried each alone at 60°C, 80°C and 105°C. Fig. 4 shows that for a temperature range between 20°C and 80°C, the RS has higher contribution than the NS in the mass loss of the mortar. This important difference can be explained by the fact that RS can store more water than the NS. For a temperature range between 80°C and 105°C, the contribution of both sands in the mass loss of mortars is almost the same. Between 80°C and 105°C, the difference in the type of sand used does not affect the mass loss of the mortar: the mass loss of the mortar is due to the new cement paste.

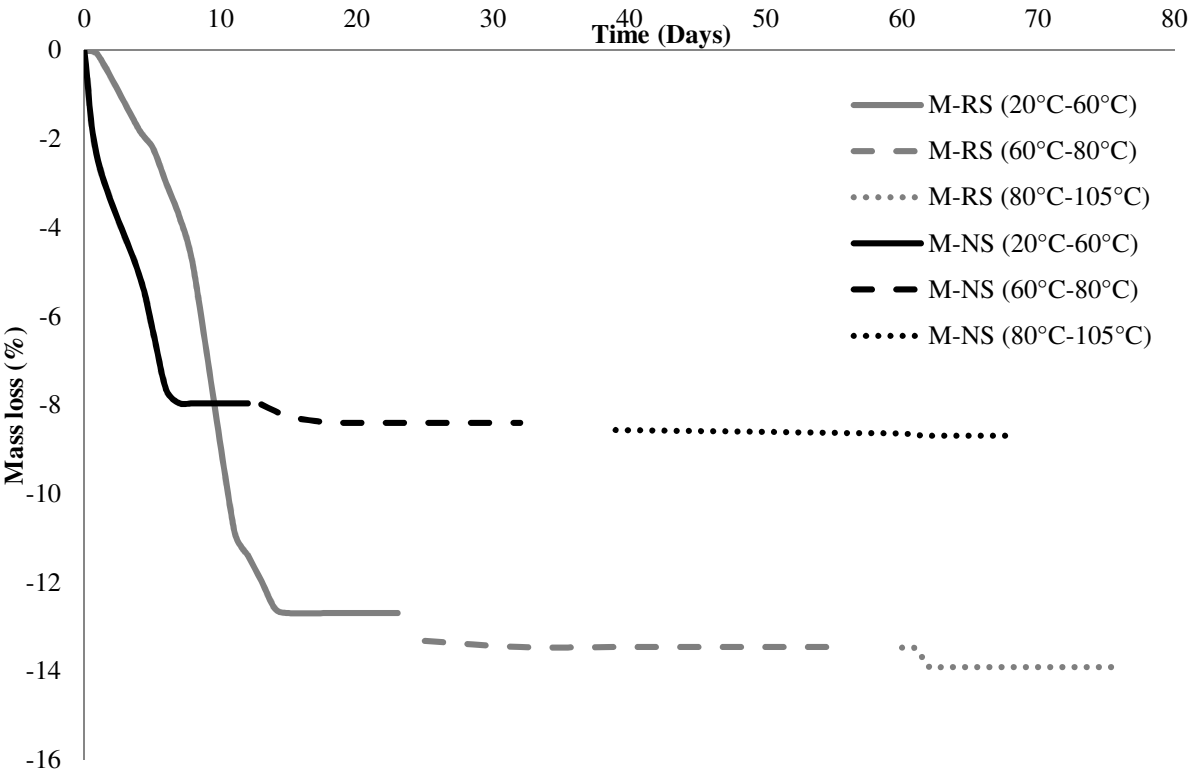

Fig. 3: Mass loss of M-RS and M-NS

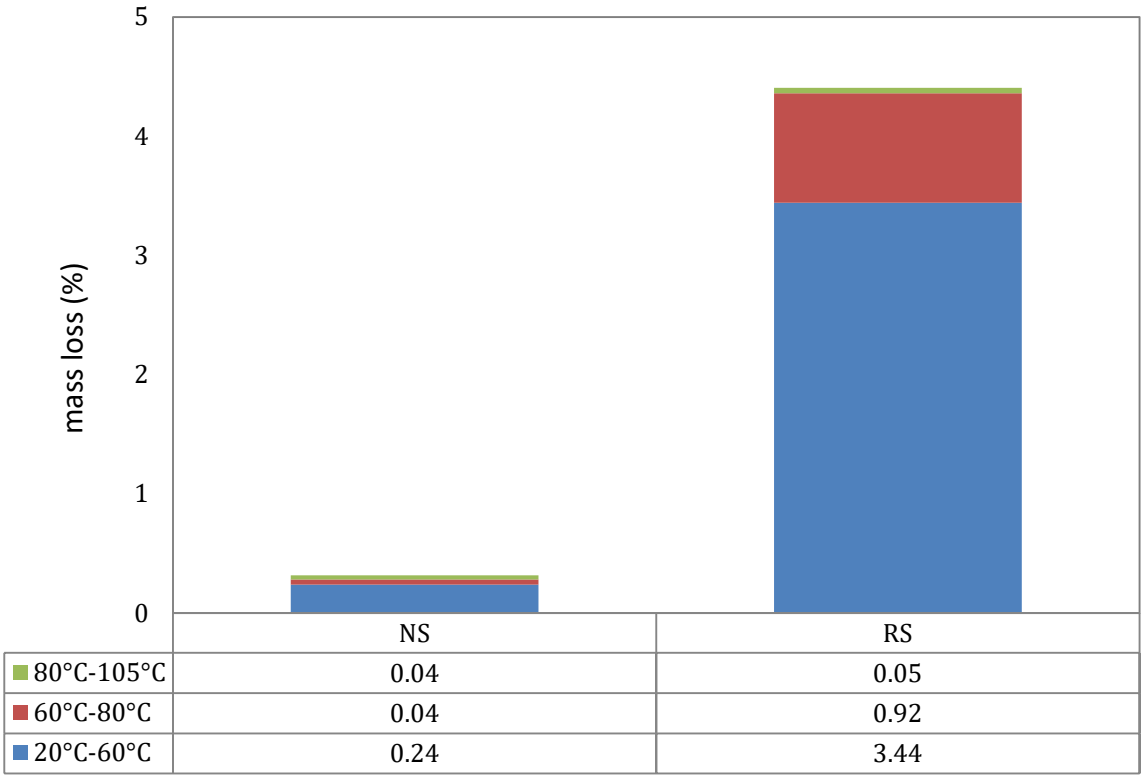

	NS	RS
80°C-105°C	0.04	0.05
60°C-80°C	0.04	0.92
20°C-60°C	0.24	3.44

Fig. 4: The mass loss of the sand at different drying temperature: mass loss (%) = $\frac{M_{Tfinal}}{M_{Tinitial}} \times 100$

	M-RS	M-NS
20°C-60°C	12.68%	7.95%
60°C-80°C	0.88%	0.48%
80°C-105°C	0.53%	0.32%
20°C-105°C	**13.9%**	**8.68%**

Table 4: Relative mass loss ΔM (%) of mortars made of RS and NS

4.2 Effect of the temperature on water porosity (P)

Fig. 5 presents the water porosity of M-NS and M-RS at different drying temperatures (60°C, 80°C and 105°C). The water porosity of M-RS is higher than M-NS; this is due to the fact that RS are more porous than NS (see Table 2). The water porosity increases with the increase of the drying temperature. The increase in water porosity between 60°C and 105°C is about 10% and 19% for M-NS and M-RS respectively. This increase in the water porosity is caused by the departure of the water between 60°C and 105°C and/or a change in the microstructure of mortars due to the elevated temperature. The relative mass loss ΔM between 60°C and 105°C is calculated in Table 4 and it is found to be 0.8% and 1.4% for M-NS and M-RS respectively. In that case, which type of water is responsible for the increase in the water porosity? Is it the free water or the bound water? According to Fig. 4, the contribution of the sands in the mass loss of the mortar between 80°C and 105°C is almost null. Whereas the contribution of the sands between 60°C and 80°C is much higher in the case of RS. The increase in the water porosity of mortars is due to the evaporation of the free water in the aggregates. RS is more porous than NS; so it can stock more free water in its porosity that affects more the temperature dependence of the water porosity of the mortar.

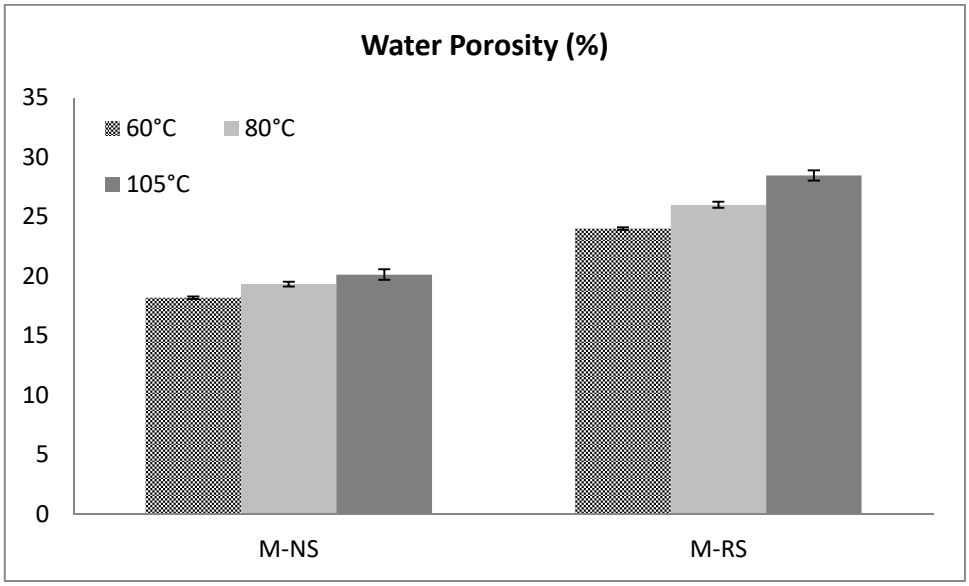

Fig. 5: Water porosity of mortars at different drying temperatures

4.3 Effect of temperature on the intrinsic permeability (K_{int})

After measuring the water porosity, the same specimen undergoes the gas permeability test. Fig. 6 put in evidence that the intrinsic permeability coefficient (K_{int}) of M-NS and M-RS increases with the increase of the drying temperature. This increase in K_{int} is more significant in the case of M-RS. The increase for the M-NS dried between 60°C and 105°C is about 12.2% where as an increase of 28.4% is noticed in the case of M-RS. The gas permeability of M-RS is also always higher than M-NS [25]. This is consistent with the high porosity and the high water absorption coefficient of the RS compared to NS (Table 2). Mortar is a capillary porous material and its permeability is related to its microstructure. According to [14], the microstructure change starts to take place at 80°C, so the increase of K_{int} with the increase of the drying temperature could be due to the microstructure damage. The increase in K_{int} is higher in the case of M-RS. M-RS undergoes more damage than the M-NS, which creates favorable passages for gas flow. The gas flow increases through cracks created by the elevated temperature.

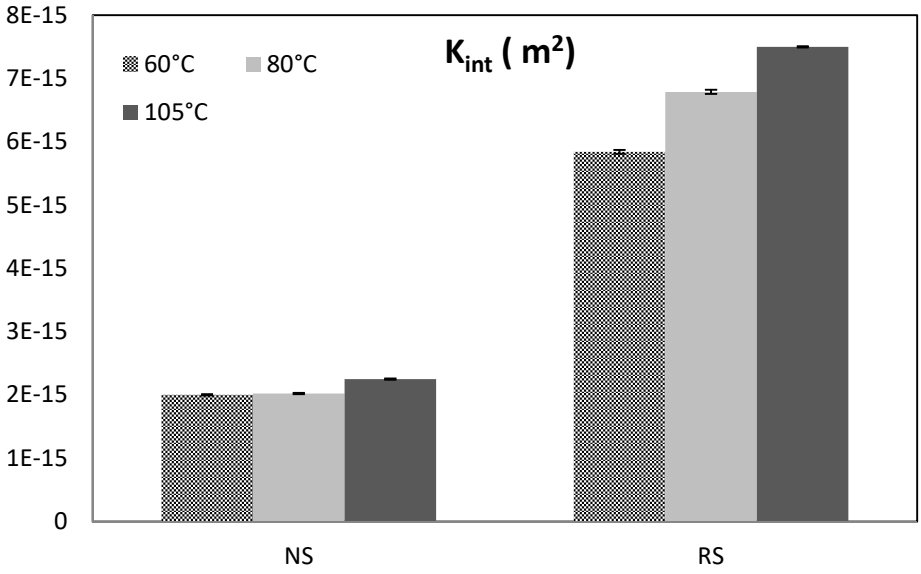

Fig. 6: Gas permeability of mortars at different drying temperatures

4.4 Relationship between ΔM and the change in water porosity (Pt/P0)

The change in the water porosity Pt/P0 is defined as the ratio between the water porosity of mortar at a given temperature (Pt) and the water porosity of the undamaged mortar (P0). In this section, we assume that the undamaged mortar is the one dried at 60°C. At 60°C, and according to the literature review, we are sure that the temperature does not cause any damage or change to the microstructure of cementitious materials [26]. The change in the water porosity can be related to the variation of mass (ΔM) calculated in Fig. 3 and Table 4. Fig. 7 presents the evolution of the water porosity with ΔM. We notice that the mass loss and the change in water porosity follow a linear relation both types of mortars, the slope of which is almost the same for both types of sand between 60°C and 105°C.

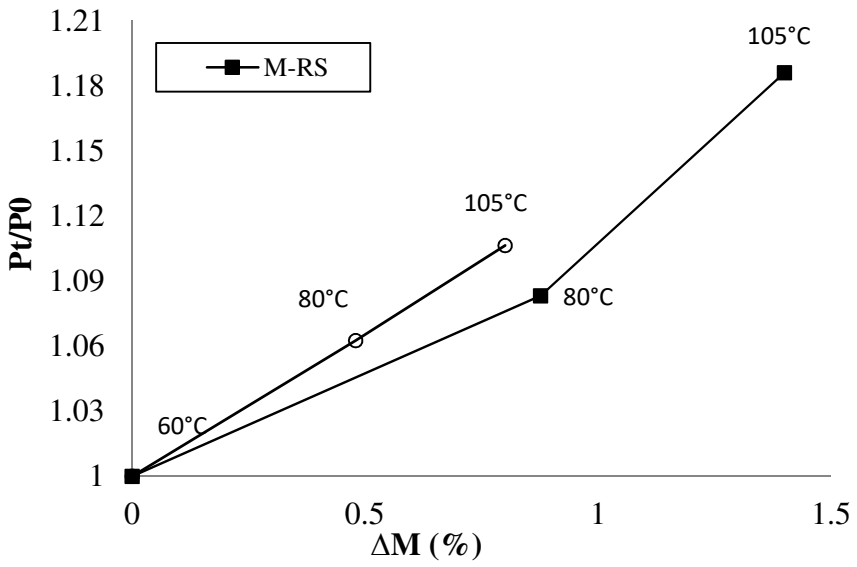

Fig. 7: The evolution of the change in water porosity with respect to percentage mass loss

4.5 Relationship between ΔM and the change in gas permeability (Kt/K0)

The change in gas permeability is defined as the ratio between the gas permeability of mortar at a given temperature (Kt) and gas permeability of the undamaged mortar (K0) at 60°C. The change in gas permeability can be related to the variation of mass (ΔM) calculated in Fig. 3 and Table 4. Fig. 8 presents the evolution of the gas permeability with the ΔM. We notice that contrary to the water porosity, the change in gas permeability of mortars does not vary at the same rate in function of ΔM. For M-RS, the variation is linear whereas in the case of M-NS the variation looks like parabolic. We can notice that the slope of the M-RS between 60°C and 80°C is much higher than the one of the M-SN and that between 80°C and 105°C it is almost identical. According to Fig. 4, between 80°C and 105°C, the sand does not contribute much in the mass loss of mortars whereas Fig. 8 shows that K_{int} increases significantly in the case of both sands. We can explain this increase of K_{int} by the micro-cracks created in the new cement paste and in the RS at temperature higher than 60°C.

The gas flow is highly affected by the mass loss of the sand (which is higher in the case of RS) between 20°C and 80°C, whereas between 80°C and 105°C is controlled by the new cement

paste, which explains why the slope of the Kt/K0 vs ΔM curves of M-RS and M-NS are almost identical. The evaporation of the free water is not the only reason affecting the gas permeability properties of M-RS. The increase in the drying temperature leads to an increase in the pores connectivity in the microstructure of M-RS due to damage.

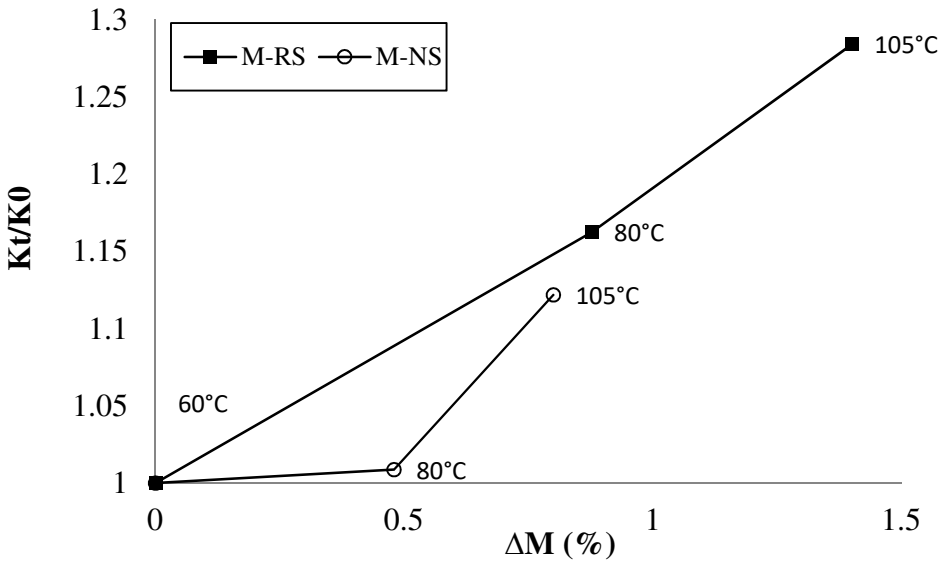

Fig. 8: The evolution of the change in gas permeability with respect to percentage mass loss

4.6 Relationship between the gas permeability and damage coefficient

Many studies were conducted in order to determine the effect of presence of cracks on the permeability of concrete [22,27–29]. It was found that the gas permeability changes very significantly with the increase of damage level. The dynamic modulus of elasticity is measured at 20°C (before drying) and at 60°C, 80° and 105°C. The same specimen is used for all the measurements. It can be noticed that the dynamic modulus of elasticity decreases with the increase of the drying temperature (Table 5). This is due to the evaporation of water that increases the wave propagation speed. The results of the dynamic modulus of elasticity obtained are shown in Table 5.

	20°C	60°C	80°C	105°C
M-NS	27.008	21.456	18.822	16.31
M-RS	14.018	10.558	8.967	7.236

Table 5: The dynamic Young modulus of mortars in GPa

Fig. 9 shows the increase of $K_{int}/K0$ with the damage value evaluated by the dynamic method. The damage value D of M- RS is higher than the one of M-NS (Table 5). We notice that the relationship between $K_{int}/K0$ and D can be expressed as an increasing linear function in the case of M-RS. In the case of M-NS, the slope of the relationship between $K_{int}/K0$ and D between 60°C and 80°C is almost nonexistent, whereas between 80°C and 105°C, we notice an increase in D. This result is similar to the one obtained in Fig. 8. We can assume that for a temperature range between 60°C and 80°C, the elevated temperature creates more cracks in M-RS than in M-NS (higher values of D) allowing the gas to flow better through the cracks. Between 80°C and 105°C, the damage created by the high temperature is identical for both types of mortars.

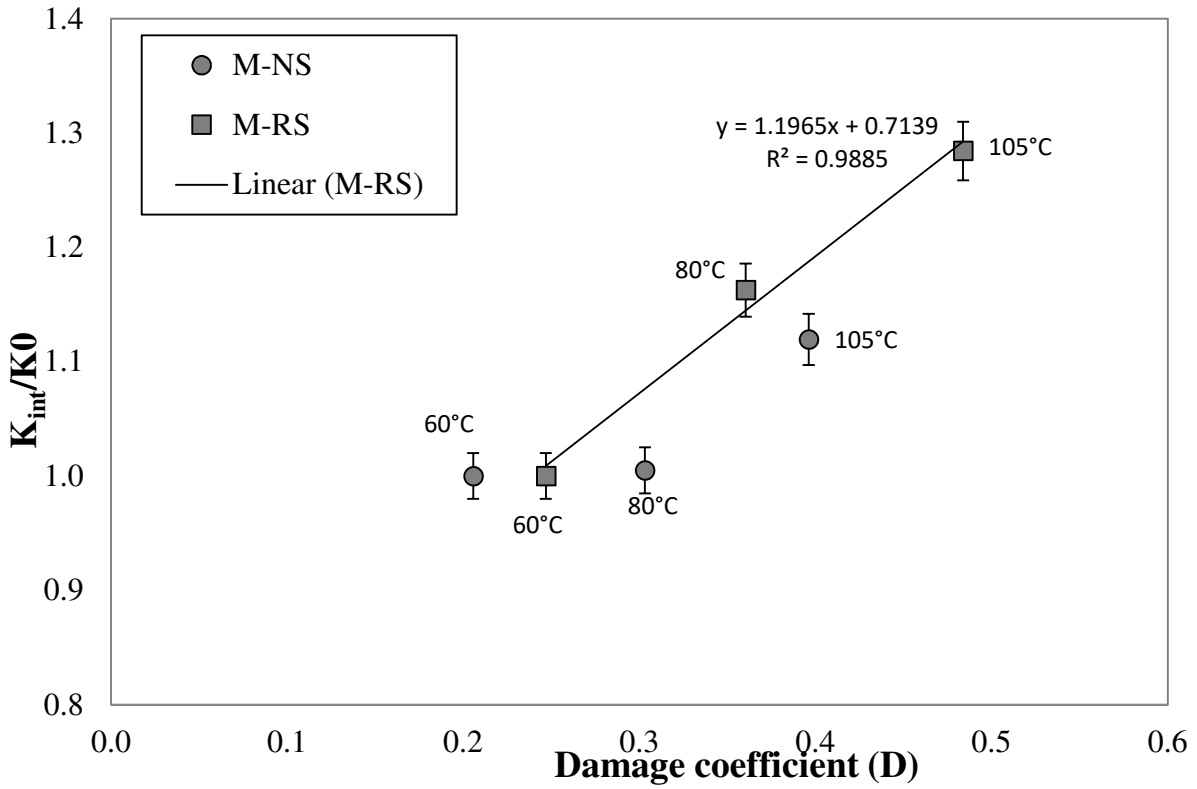

Fig. 9: Relationship between gas permeability and damage coefficient

4.7 Discussion

Literature review results along with the results obtained during this research are summarized in Table 5. Gas permeability and water porosity tests are not done at 20°C since it is the ambient temperature and no major evaporation happens at this range of temperature. According to many studies done in this subject, the evaporation of water in mortar and concrete depends on the temperature ranges. At 20°C-60°C, we notice the evaporation of the free water, thus no damage in the microstructure is observed. Whereas for temperatures above 60°C, the bound water starts to evaporate [10,11,13,14,22,24]; this is due to the dehydration of the C-S-H gel and ettringite causing damage in the microstructure that worsens with the increase of temperature. This damage of microstructure is confirmed by the damage factor (D) calculated using the Young dynamic modulus after drying at the desired temperature. This damage value is higher in the case of M-RS resulting in an important increase in the K_{int} of the mortar. This is due to the fact that the RS contains 20-25% in mass more adherent cement paste [6–9] in addition to the new cement added during the fabrication of mortar. Thus, M-RS are more sensible to high temperature.

In this paper, we found that increasing the drying temperature from 60°C to 105°C does not influence the water porosity of M-RS as much as its gas permeability. Between 60°C-80°C, an important difference is noticed in the gas permeability (K_{int}) for M-RS. The K_{int} increased by 16.24% where the change is only 0.87% for M-NS. The ΔM for both specimens does not exceed 1%. Thus, this increase in K_{int} proves that a major change in the microstructure of M-RS happened. Micro-cracks appear with a drying temperature above 60°C creating favorable passages to the gas flow throughout the M-RS. At 105°C, a similar increase in the K_{int} values is noticed for both mortars. This is due to the dehydration of the C-S-H gels and the ettringite in the new cement paste causing the escape some of the bound water. The sand used here plays a minor role in the mass loss of the mortar because NS and RS have approximately the same

contribution in the mass loss of mortars (Fig. 4). The evaporation of the bound water damages the microstructure of mortars and micro-cracks appear causing the increase in the gas permeability.

Accordingly, the choice of the drying temperature to pre-treat the specimens before investigating durability properties is important; the temperature imposed by standard methods (105°C) is not suitable for cementitious materials in general and its effect is more serious in the case of M-RS. An important damage starts to appear for a temperature range above 60°C for M-RS and above 80°C for M-NS. In order to make sure that the microstructure of M-RS is not damaged and the durability results are not affected, we suggest drying at 60°C until a constant mass.

Temperature		20°C-60°C	60°C-80°C	80°C-105°C
Evaporation of		Free water [22]	Free water + bound water of C-S-H [10, 12, 21, 26]	
Damage		NO [22, 24]	YES [26]	
			Changes in microstructure[26]	Major changes in microstructure [25]
ΔM (%)	M-NS	7.95%	0.48%	0.32%
	M-RS	12.68%	0.88%	0.53%
ΔP (%)	M-NS	-	6.263%	4.136%
	M-RS	-	8.333%	9.5%
ΔK_{int} (%)	M-NS	-	0.871%	11.231%
	M-RS	-	16.243%	10.456%
D	M-NS	0.206	0.303	0.396
	M-RS	0.246	0.360	0.484

Table 6: Summary of the results obtained

5. Conclusion

In this study, for a total replacement of NS by RS, a relationship between mass loss, water absorption and durability properties (gas permeability and damage coefficient) has been established. Therefore, the following conclusions can be drawn from the test results and discussions in this paper:

- M-RS presents water porosity and gas permeability higher than M-NS and a smaller dynamic Young modulus; this is due to the high porosity of RS and the adherent cement paste.
- Increasing the drying temperature from 60°C to 105°C does not influence the water porosity of M-RS as much as the gas permeability.
- The increase in the gas permeability between 60°C and 105°C is not only due to the evaporation of free water. By increasing the drying temperature, bound water between C-S-H gels starts to evaporate damaging the microstructure of the mortar; micro-cracks can appear, these micro-cracks increase the gas permeability of M-RS.
- In the case of drying mortar made of RS, the pre-treatment should be preferably done at 60°C, and not at 105°C as recommended by the standard methods, to avoid any microstructural change in the specimen.
- Although the standards methods recommend the drying at 105°C for ordinary mortars, we found that for a temperature range above 80°C can cause serious damage in the microstructure of the mortar. The drying of the ordinary mortar should be preferably done at 80°C until constant mass.
- The mass loss of mortar and the contribution of the sand in this mass loss can be used in modelling to predict the evolution of the P and K_{int} for each temperature range (60°C-80°C and 80°C-105°C).

In conclusion, the results obtained are indicative and specific to mortars made of recycled sand and cannot be generalized to recycled aggregate concrete. Additional experimental programs need to be established as ITZ studies, replacement degree and the use of the coarse fraction of the RCA, in order to generalize the conclusion obtained.

References

[1] C.. Poon, Z.. Shui, L. Lam, Effect of microstructure of ITZ on compressive strength of concrete prepared with recycled aggregates, Constr. Build. Mater. 18 (2004) 461–468. doi:10.1016/j.conbuildmat.2004.03.005.

[2] M. Casuccio, M.C. Torrijos, G. Giaccio, R. Zerbino, Failure mechanism of recycled aggregate concrete, Constr. Build. Mater. 22 (2008) 1500–1506. doi:10.1016/j.conbuildmat.2007.03.032.

[3] L. Butler, J.S. West, S.L. Tighe, The effect of recycled concrete aggregate properties on the bond strength between RCA concrete and steel reinforcement, Cem. Concr. Res. 41 (2011) 1037–1049. doi:10.1016/j.cemconres.2011.06.004.

[4] J. Xiao, W. Li, Y. Fan, X. Huang, An overview of study on recycled aggregate concrete in China (1996–2011), Constr. Build. Mater. 31 (2012) 364–383. doi:10.1016/j.conbuildmat.2011.12.074.

[5] NF EN 206+A1 : "Béton-Specification, performances, production et conformité," (2016).

[6] M.S. de Juan, P.A. Gutiérrez, Study on the influence of attached mortar content on the properties of recycled concrete aggregate, Constr. Build. Mater. 23 (2009) 872–877. doi:10.1016/j.conbuildmat.2008.04.012.

[7] R. Zaharieva, F. Buyle-Bodin, F. Skoczylas, E. Wirquin, Assessment of the surface permeation properties of recycled aggregate concrete, Cem. Concr. Compos. 25 (2003) 223–232. doi:10.1016/S0958-9465(02)00010-0.

[8] A. Abbas, G. Fathifazl, B. Fournier, O.B. Isgor, R. Zavadil, A.G. Razaqpur, S. Foo, Quantification of the residual mortar content in recycled concrete aggregates by image analysis, Mater. Charact. 60 (2009) 716–728. doi:10.1016/j.matchar.2009.01.010.

[9] S.C. Angulo, C. Ulsen, V.M. John, H. Kahn, M.A. Cincotto, Chemical–mineralogical characterization of C&D waste recycled aggregates from São Paulo, Brazil, Waste Manag. 29 (2009) 721–730. doi:10.1016/j.wasman.2008.07.009.

[10] M. Quattrone, B. Cazacliu, S.C. Angulo, E. Hamard, A. Cothenet, Measuring the water absorption of recycled aggregates, what is the best practice for concrete production?, Constr. Build. Mater. 123 (2016) 690–703. doi:10.1016/j.conbuildmat.2016.07.019.

[11] J. Castro, D. Bentz, J. Weiss, Effect of sample conditioning on the water absorption of concrete, Cem. Concr. Compos. 33 (2011) 805–813. doi:10.1016/j.cemconcomp.2011.05.007.

[12] J. Piasta, Z. Sawicz, L. Rudzinski, Changes in the structure of hardened cement paste due to high temperature, Matér. Constr. 17 (1984) 291–296. doi:10.1007/BF02479085.

[13] H.F.W. Taylor, Cement Chemistry, 2nd ed., Thomas Telford, London, 1997.

[14] Q. Zhou, F.P. Glasser, Thermal stability and decomposition mechanisms of ettringite at <120°C, Cem. Concr. Res. 31 (2001) 1333–1339. doi:10.1016/S0008-8846(01)00558-0.

[15] A. Yacoub, A. Djerbi, T. Fen-Chong, Water absorption in recycled sand: New experimental methods to estimate the water saturation degree and kinetic filling during mortar mixing, Constr. Build. Mater. 158 (2018) 464–471. doi:10.1016/j.conbuildmat.2017.10.023.

[16] NF EN 1097-6, Tests for mechanical and physical properties of aggregates - part 6: determination of particle density and water absorption, (2014).

[17] Z. Zhao, S. Rémond, D. Damidot, W. Xu, Influence of hardened cement paste content on the water absorption of fine recycled concrete aggregates, Journal of Sustainable Cement-Based Materials, 2 (2013), 186-203.

[18] EN 196-1, Methods of testing cement - Part 1: Determination of strength, (2006). European Committee for Standardization.

[19] NF P18-459, Concrete - Testing hardened concrete - Testing porosity and density, (2010).

[20] J.J. Kollek, The determination of the permeability of concrete to oxygen by the Cembureau method—a recommendation, Mater. Struct. 22 (1989) 225–230. doi:10.1007/BF02472192.
[21] L.J. Klinkenberg, The Permeability of Porous Media To Liquids and Gases, API Drill. Prod. Pract. (1941) 200–213.
[22] A. Djerbi Tegguer, S. Bonnet, A. Khelidj, V. Baroghel-Bouny, Effect of uniaxial compressive loading on gas permeability and chloride diffusion coefficient of concrete and their relationship, Cem. Concr. Res. 52 (2013) 131–139. doi:10.1016/j.cemconres.2013.05.013.
[23] R.F. Feldman, V.S. Ramachandran, Differentiation of interlayer and adsorbed water in hydrated Portland cement by thermal analysis, Cem. Concr. Res. (1971) 607–620.
[24] M.C.R. Farage, J. Sercombe, C. Gallé, Rehydration and microstructure of cement paste after heating at temperatures up to 300 °C, Cem. Concr. Res. 33 (2003) 1047–1056. doi:10.1016/S0008-8846(03)00005-X.
[25] C. Thomas, J. Setién, J.A. Polanco, P. Alaejos, M. Sánchez de Juan, Durability of recycled aggregate concrete, Constr. Build. Mater. 40 (2013) 1054–1065. doi:10.1016/j.conbuildmat.2012.11.106.
[26] M. Lion, F. Skoczylas, Z. Lafhaj, M. Sersar, Experimental study on a mortar. Temperature effects on porosity and permeability. Residual properties or direct measurements under temperature, Cem. Concr. Res. 35 (2005) 1937–1942. doi:10.1016/j.cemconres.2005.02.006.
[27] C. Zhou, K. Li, J. Han, Characterizing the effect of compressive damage on transport properties of cracked concretes, Mater. Struct. 45 (2012) 381–392. doi:10.1617/s11527-011-9771-4.
[28] M. Choinska, A. Khelidj, G. Chatzigeorgiou, G. Pijaudier-Cabot, Effects and interactions of temperature and stress-level related damage on permeability of concrete, Cem. Concr. Res. 37 (2007) 79–88. doi:10.1016/j.cemconres.2006.09.015.
[29] V. Picandet, A. Khelidj, G. Bastian, Effect of axial compressive damage on gas permeability of ordinary and high-performance concrete, Cem. Concr. Res. 31 (2001) 1525–1532. doi:10.1016/S0008-8846(01)00546-4.